SCIENTIFIC REPORTS
nature research

OPEN

Ultrasensitive nano-aptasensor for monitoring retinol binding protein 4 as a biomarker for diabetes prognosis at early stages

Raheleh Torabi[1] & Hedayatollah Ghourchian[1,2*]

Prognosis of diabetes risk at early stages has become an important challenge due to the prevalence of this disease. Retinol binding protein 4 (RBP4), a recently identified adipokine, has been introduced as a predictor for the onset of diabetes type 2 in coming future. In the present report a sensitive aptasensor for detection of RBP4 is introduced. The immune sandwich was prepared by immobilizing biotinylated RBP4 aptamers on streptavidin coated polystyrene micro-wells and then incubation of RBP4 as target and finally addition of luminol-antibody bearing intercross-linked gold nanoparticles as reporter. The chemiluminescence intensity was recorded in the presence of hydrogen peroxide as oxidant agent and Au^{3+} as an efficient catalyst for luminol oxidation. The aptasensor responded to RBP4 in the linear concentration range from 0.001 to 2 ng/mL and detection limit was slightly less than 1 pg/mL. The proposed method has successfully applied to determine the RBP4 in patient real serums. By using the intercross-linked gold nanoparticles, it is possible to provide more accessible surface for immobilizing luminol and enhance the chemiluminescence signal. Therefore, the analytical parameters such as sensitivity, specificity, detection limit and linear range were improved in compare to the biosensors reported in the literature.

Type 2 diabetes (T2D) has become a major challenge for public health worldwide. Increasing the prevalence of T2D could be due to the factors such as aging, urbanization, obesity, physical inactivity and modern lifestyle. Among them, obesity contributes in insulin resistance and abnormal glucose metabolism[1]. T2D can lead to many serious complications including cardiovascular, kidney and eye diseases and nerve damages as well. These diseases eventually may lead to premature death[2–4]. Moreover, treatment of T2D and its complications cost billion dollars per year for health care and also indirect costs caused by loss of productivity from disability and early mortality[5]. Accordingly, preventing or delaying the diabetes will improve the quality of individual life via reducing the diabetes-related complications. In recent years several various gene and protein biomarkers including retinol binding protein 4 (RBP4) have been introduced for prognosis of T2D[6]. RBP4 has been introduced as an independent predictive biomarker at early stages of insulin resistance[7]. The blood serum levels of RBP4 correlates significantly with other major factors related to insulin resistance such as triglyceride, cholesterol and blood pressure. Explaining the mechanism for the relation of elevated RBP4 with the risk of insulin resistance and T2D is complex due to the dark aspects of this process[8]. High fat storage in adipose tissues elevates the levels of RBP4 by which the expression of the insulin-stimulated glucose-transporter4 (GLUT4) in adipocytes is selectively reduced and consequently leads to decrease glucose uptake. In addition, increasing the level of RBP4 in blood serum might contribute to impair insulin-stimulated glucose uptake in muscle by decreasing enzyme PI-3 kinase activity. However, in liver, it can elevate hepatic glucose production by stimulating phosphoenol pyruvate carboxy kinase expression which is the characteristics of T2D[9]. An early study in 2014 has shown that RBP4 directly induces macrophages to secrete proinflammatory cytokines which results in greater inflammation in adipose tissue and insulin resistance[10]. Thus, these various effects of elevated level of RBP4 can lead to insulin resistance before any significant changes in diabetic markers in high risk population[11]. So, the elevation of RBP4 level can be a sign for catching the diabetes.

[1]Laboratory of Bioanalysis, Institute of Biochemistry and Biophysics, University of Tehran, Tehran, Iran. [2]Nanobiomedicine Center of Excellence, Nanoscience and Nanotechnology Research Center, University of Tehran, Tehran, Iran. *email: ghourchian@ut.ac.ir

So far, various methods including ELISA (enzyme-linked immunosorbent assay) and conventional antibody-based assays have been presented for the quantitative measurement of human RBP4[12]. However, for improving specific detection and precise quantification of RBP4, aptamers were used. Aptamers are synthetic single-stranded oligonucleotides with high specificity and affinity to their targets that make them ideal candidates for molecular recognition systems[13]. Aptamers have been applied in biosensor design (aptasensor) due to their advantages over antibodies including: stability, availability, modifiability, flexibility and in some cases better specificity and affinity than similar antibodies[14]. RBP4 binding aptamer (RBA) is a 76-bp ssDNA sequence with very low Kd value ($0.2 \pm 0.03\,\mu M$)[15]. The specificity of this aptamer (RBA) has already been confirmed by using Vaspin, Nampt, adiponectin (ADPN), human serum albumin (HSA), human IgG and fibrinogen as negative controls[16]. RBA has also been applied in the enzyme-linked antibody-aptamer sandwich system with colorimetric reaction for more convenient and sensitive detection of RBP4 (78 ng/mL)[16].

In the present study, an ultrasensitive aptasensor has been designed for the assessment of human RBP4 level in blood serum. In this system, RBP4 has been captured by immobilized RBA on plate and then detected by polyclonal luminol-antibody bearing intercross-linked gold nanoparticles (GNPs). GNPs were intercross-linked to each other via cysteine as a simple and low cost linker. Such big clusters increased the accessible surface for conjugating polyclonal antibodies and luminol molecules. Consequently, the efficient conjugation of polyclonal antibodies increased the probability of antibody-antigen interaction and on the other hand, the proficient conjugation of luminol molecules on GNP clusters could amplify the chemiluminescence signals. To our knowledge, there is no report applying RBA in chemiluminescent aptasensor. Application of chemiluminescence as a highly sensitive physical transducer together with the luminol-antibody bearing intercross-linked GNPs, will level up the aptasensor signal to an ultrasensitive scale.

Results

Characterization of GNPs. For single and intercross-linked GNPs characterization, the nanoparticle suspension was diluted in deionized water. The diameter of diluted single GNPs was measured by DLS to be in the range from 18 to 28 nm, while that for intercross-linked GNPs was in the range from 28 to 40 nm. These values were also confirmed by the images obtained by transmission electron microscopy (Fig. 1a–c).

The extinction coefficient (ε) for GNPs was calculated according to Eq. 1[17]:

$$\mathrm{Ln}\,\varepsilon = \mathrm{k}\,\mathrm{ln}\,\mathrm{D} + \mathrm{a} \tag{1}$$

where, D (nm) is the average diameters of the nanoparticles, k and a, were 3.32 and 10.8, respectively. Then, according to the OD_{570} calculated using the Eq. 2[17], the single and intercross-linked GNPs concentrations were estimated to be 1.56×10^{-6} and 1.7×10^{-9} M, respectively:

$$\mathrm{OD} = \varepsilon \mathrm{C} \tag{2}$$

Intercross-linking of GNPs was also confirmed by using UV-Vis spectroscopy. In Fig. 1d, the absorption peak for GNPs (530 nm), intercross-linked GNPs (560 nm) and luminol-antibody bearing cross-linked GNPs (570 nm) have been compared. As seen after cross linking of GNPs the absorption peak was flattened and shifted to right owing to increase in particle size[18]. By immobilization of antibody and luminol on GNPs, the UV-Vis absorption peak was even shifted in some extend.

ATR-FTIR Spectroscopy was performed to characterize the intercross-linkage of GNPs. Since no characteristic absorption peak was observed for free -SH at 2559 cm^{-1}, one may conclude that the free -SH groups in MUA and cysteine have already been bound onto GNPs surface. The characteristic peaks of –COOH vibrations at 1725 cm^{-1} and the saturated alkyl stretching vibration at 2867 and 2918 cm^{-1} were also indicated the presence of MUA onto GNPs surface. The peak at 1641 cm^{-1} (C=O stretching amides), the signal at 3400 cm^{-1} (–NH stretching amide) and the peak at 1350 cm^{-1} (C–N) prove the formation of (C–NH) amide bond via reaction between the primary amine groups of cysteine and the carboxylic groups of the MUA. The peaks at 760 and 1200 cm^{-1} correspond to the vibration of C–S bond which confirm the cysteine conjugation. These results indicate the formation of GNPs intercross-linked.

Effect of pH and ionic strength on the sensor response. The ability of the aptasensor for RBP detection in a wide range of pH in PBS and carbonate buffers was investigated while the chemiluminescence signals were measured. The obtained data showed that the aptasensor reached to its maximum working sensitivity in 0.02 M PBS buffer at pH 8.0.

To optimize ionic strength, the sensor response was recorded in PBS containing different NaCl concentrations (50, 100,150, 200 mM). The maximum signal was obtained in 0.02 M PBS (pH 8) containing 100 mM NaCl.

Signal amplification by intercross-linked GNPs. In order to assess the ability of intercross-linked GNPs in signal amplification, the chemiluminescence intensity resulted from luminol-antibody bearing GNPs was compared with that obtained from luminol-antibody bearing intercross-linked GNPs. As shown in Fig. 2a, the intercross-linked GNPs exhibited more than 24 times chemiluminescence intensity relative to the GNPs.

Application of luminol bearing nanoparticles for creating stable and strong signals is common in chemiluminesence biosensors. In the most of reports, antibodies are conjugated to luminol bearing GNPs covalently through the interactions between AuNPs and either mercapto or primary amine groups of biomolecules via Au-S and Au-N bonds. However, some research groups attempted to use the branched luminol bearing GNPs for increasing the sensitivity and enhancing the signal[19]. But in the present study, GNPs were intercross-linked to each other via Cys as a simple and low cost linker (Fig. 3F). As shown in Fig. 1c, at higher concentrations of cysteine, the GNPs intercrossed each other and formed the clusters with the diameters around 67 nm. Such

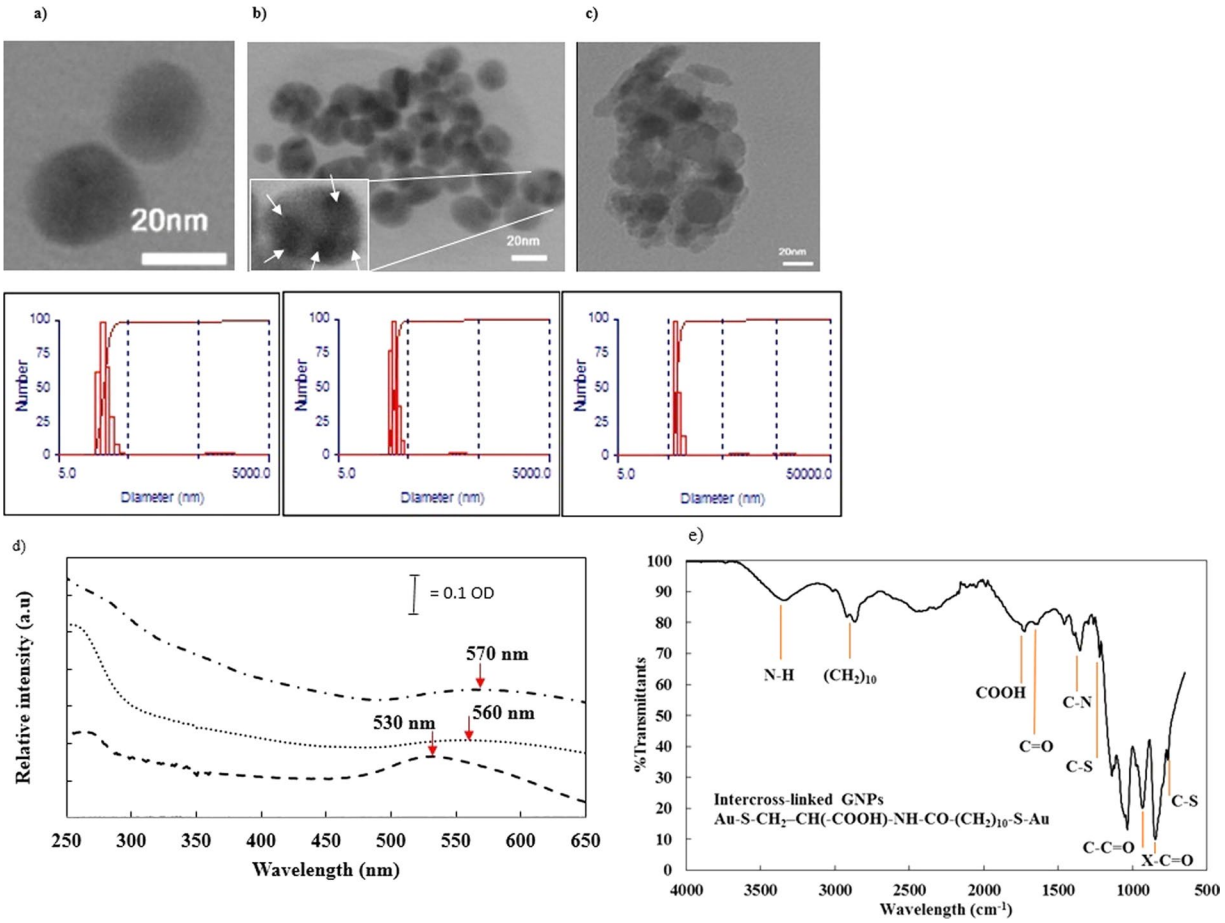

Figure 1. Transmission electron microscopy (TEM) images of three types of GNPs: (**a**) single GNPs and intercross-linked GNPs at (**b**) lower and (**c**) higher concentration of cysteine bearing GNPs. As shown in the lower part of images, the mean diameter obtained by DLS for (**a**, **b** and **c**) are 22.5, 31.7 and 67 nm, respectively. (**d**) UV-Visible spectroscopy of 20 nm-GNPs (Dashed line, Peak: 530 nm), cross-linked GNPs (Dotted line, Peak: 560 nm) and luminol-antibody bearing cross-linked GNPs (Dash-dotted line, Peak: 570 nm). (**e**) FT-IR spectrum of intercross-linked GNPs.

big clusters increased the accessible surface for conjugating polyclonal antibodies and luminol molecules. Consequently, the efficient conjugation of polyclonal antibodies increased the probability of antibody-antigen interaction and on the other hand, the proficient conjugation of luminol molecules on the GNP clusters could amplify the chemiluminescence signals.

In 2005, Zhang *et al.* introduced a three steps mechanism for chemiluminescence signal production by luminol: oxidation of luminol to luminol radical and then oxidation of the luminol radical to a key intermediate followed by decomposition of hydroxyl hydroperoxide with the emission of chemiluminescence. Here we emphasize on the enhancement of chemiluminescence by GNPs in a luminol-H_2O_2 system. It is supposed that GNPs can facilitate the radical generation and then the electron-transfer process is taking place at the surface of GNPs[20,21]. Moreover, in our previous work[22] it has been shown that gold even in ion form can act as an efficient catalyst for luminol oxidation and consequently increases the intensity of chemiluminescence signal. Entirely, all of these strategies resulted to creating extremely high chemiluminescence signals and increasing sensitivity to femto-gram level.

Stability. The stability of luminol-antibody bearing intercross-linked GNPs was investigated by monitoring the chemiluminescence intensity of 10 µl of 0.5 nM GNPs in PBS (pH 8.0) solution during 21 days while the solution was kept at 4 °C in dark. Comparison of the chemiluminescence signals revealed that 95% of the initial intensity was retained after a 21-day storage period.

Specificity. Figure 2b compares the specificity of aptasensor towards RBP4 and some abundant proteins in serum including BSA, HSA, fibrinogen, insulin and also anti-RBP4 antibody as an IgG and vaspin as a protein belonged to adipokines, as well. The chemiluminescent responses of aptasensor were recorded for a laboratory made serum containing 1 ng/mL of either the main target (RBP4) or other potentially interfering proteins (BSA, HSA, fibrinogen, insulin and anti-RBP4 antibody and vaspin). The results revealed that the proposed aptasensor responded more significantly to RBP4 than the other proteins. It seems that applying both aptamer and antibody

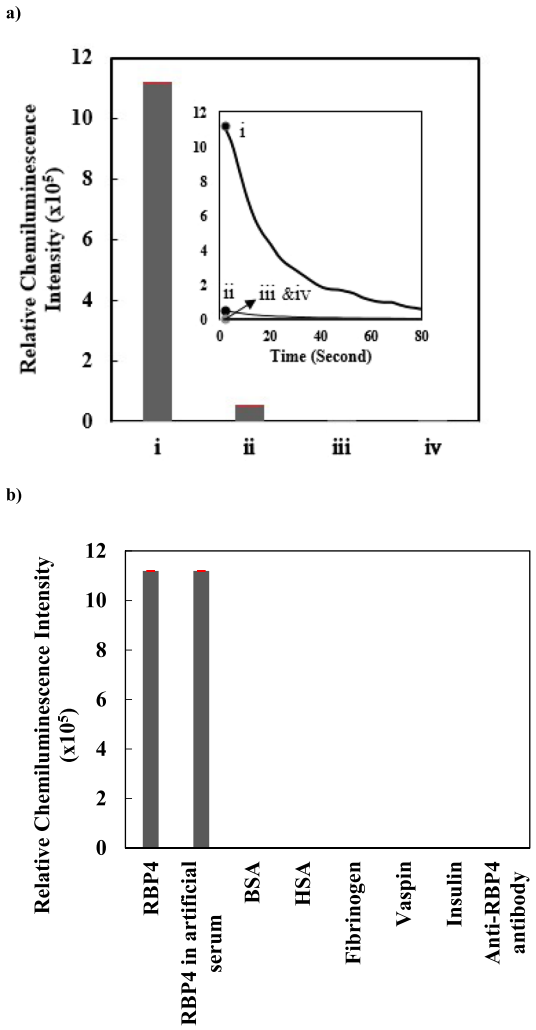

Figure 2. (**a**) Comparison between the chemiluminescence intensity obtained by aptamer/RBP4/luminol-antibody bearing intercross-linked gold nanoparticles (i) and aptamer/RBP4/luminol-antibody bearing gold nanoparticles (ii). In both tests the concentration of RBP4 was1 ng/mL. iii and iv are negative controls (Same as i and ii but, in the absence of RBP4) (**b**) Specificity of RBP4 biosensor towards different targets. Artificial serum was PBS containing 1 ng/mL of either main target (RBP4) or the other potentially interfering proteins: BSA, HSA, fibrinogen, insulin and anti-RBP4 antibody and vaspin.

improved the specific detection of RBP4. In addition, washing process in a sandwich-type procedure may have limited nonspecific binding, resulting in a low background signal. The specificity of RBA has also been previously confirmed by using Vaspin, Nampt. ADPN, HSA, human IgG and fibrinogen as negative controls[16].

Calibration curve. Under the optimized conditions, the calibration curve for determination of RBP4 was plotted. As shown in Fig. 4, the chemiluminescence intensity increased linearly with increasing RBP4 concentration in the range from 0.001 to 2 ng/mL. According to Eq. 3, the detection limit was calculated to be less than 1 pg/mL (951 fg/mL), while the standard deviation at lowest concentration was 3.479. This value was lower than the detection limit for RBP4 obtained by other techniques (Table 1) except a recently reported biosensor which applying monoclonal antibody to detect RBP4 electrochemically[23].

Feasibility of aptasensor for real samples. The feasibility of present aptasensor for real samples was assessed by 20 serum samples from normal and diabetic individuals, obtained from Tehran University of Medical Sciences. At the same time RBP4 in real samples was determined by the aptasensor and Human ELISA Kit (ab108897) and the results were compared in Tables 2–3. The values of RBP4 concentrations in the samples were obtained by using the calibration curve (Fig. 4). By comparing the results of ELISA Kit with those obtained by aptasensor, a fine consistency was achieved. The intra- and inter-coefficient of variations (%CVs) were calculated to be less than 1%. This confirmed the reproducibility of aptasensor response toward RBP4.

In addition, the experimental course for conventional ELISA takes about 3 hrs, while using the present biosensor this process would be don rapidly. Because in this approach the luminol-antibody bearing intercross-linked

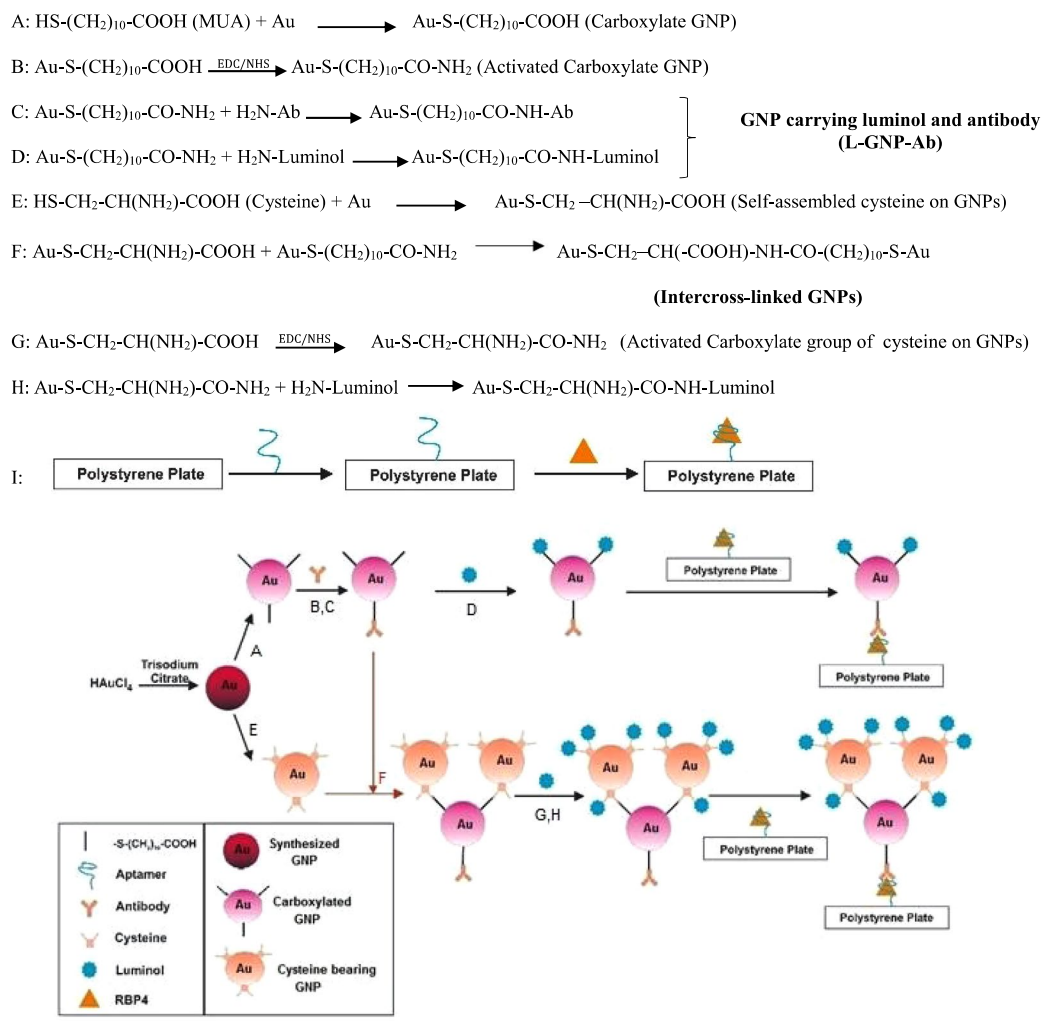

Figure 3. Steps for preparation of nano-aptasensor to monitor RBP4: (**A**) Carboxylation of GNPs via self-assembly of MUA on GNPs. (**B**) Activation of carboxylate functional group of GNPs, (**C**) Immobilization of antibody on GNPs (Ab-GNPs). (**D**) Immobilization of luminol on Ab-GNPs (L-GNP-Ab). (**E**) Self-assembly of cysteine on GNPs (Cys-GNPs). (**F**) Intercross-linking of Cys-GNPs and Ab-GNPs (GNP-Cys-GNP-Ab). (**G**) Activation of carboxylate functional group of cysteine on GNPs. (**H**) Immobilization of luminol on GNP-Cys-GNP-Ab. (**I**) Immobilization of biotinylated aptamer on streptavidin coated polystyrene micro well plate and then RBP4 protein binding to aptamer.

GNPs is prepared before starting the measurement. Moreover a simple and inexpensive laminator is used as detector of biosensor that record signals quickly. These features demonstrate the efficiency of biosensor for measuring RBP4 in real patient serums. Therefore, it seems that it has the potential to be applicable for commercial purposes.

Discussion

Obesity and accumulative fat storage increase secretion of RBP4 from adipose tissues and plasma concentration. Elevating the level of RBP4 could be a sign for early detection of T2D[11]. In the present study, an ultrasensitive aptasensor for monitoring RBP4 at the detection limit of 951 fg/mL was designed and applied for predicting diabetes at early stages. Cysteine as an available, low-cost and easy to operate linker was used for intercross-linking of GNPs. By using the intercross-linked GNPs, it was possible to provide more accessible surface for immobilizing luminol and consequently amplifying the signal. Since the luminol-antibody bearing intercross-linked GNPs was prepared before starting the measurement, the aptasensor operation became relatively fast in comparison of the most previously reported detection systems. Detection of RBP4 was carried out by formation of an immune complex via a heterogeneous interaction between aptamer-RBP4-antibody which increases the specificity of sensor[24,25]. Moreover, a simple and inexpensive laminator was used as detector of biosensor that record signals quickly. As seen in Table 1, comparing to the biosensors reported in the literature, the analytical parameters such as sensitivity, specificity, detection limit, linear range and assay time were improved. Although, the assays based on mass spectrometry have been carried out in shorter time but this method is expensive and requires well-trained personnel which is not available in usual laboratories[1,26]. Therefore, the features demonstrated in

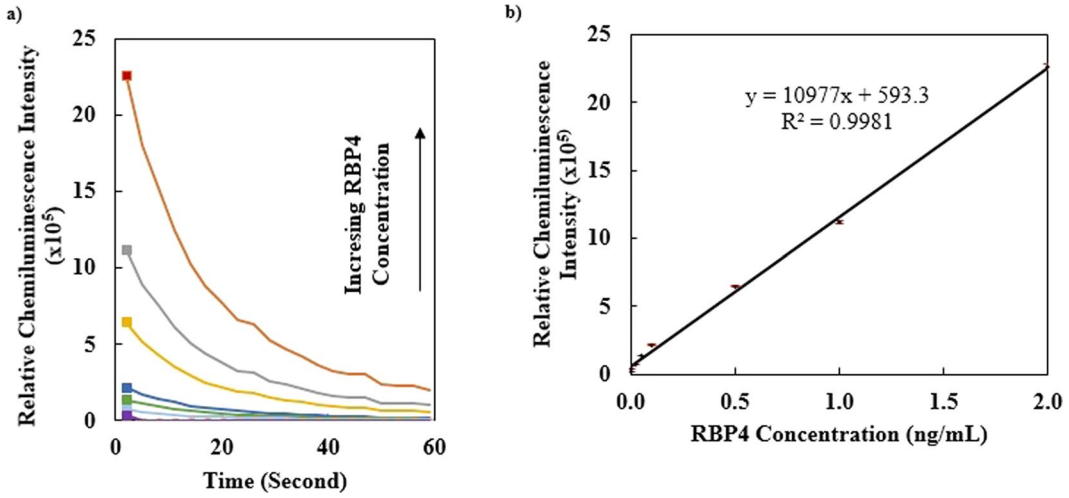

Figure 4. (**a**) Chemiluminescence intensity measurements by aptasensor in the presence of different concentrations of RBP4 (From down to up: 0, 0.001, 0.025, 0.05, 0.1, 0.5, 1 and 2 ng/mL). (**b**) Calibration curve for determination of RBP4. Each point stands for the mean value of three independent experiments.

Table 1 indicates the efficacy of aptasensor for RBP4 monitoring in real patient serums. As a result, it seems that the aptasensor has the potential to be applicable for commercial purposes, as well.

Methods

Materials and reagents. Luminol (5-amino 2,3-dihydro 1,4-phthalazinedione), H_2O_2 (30% solution) and three sodium citrate ($Na_3C_6H_5O_7$) were purchased from Merck (Germany). Gold (III) chloride hydrate ($HAuCl_4$), bovine serum albumin (BSA), human serum albumin (HSA), Fibrinogen from human plasma, 1-ethyl-3-(3-dimethylaminopropyl) carbodiimidehydrochloride (EDC), N-hydroxysuccinimide (NHS), 11-mercapto undecanoic acid (MUA), 2-morpholinoethansulfonic acid monohydrate (MES), nonionic surfactant polyoxyethylene-20 sorbitanmonolaurate (Tween-20) and absolute ethanol were purchased from Sigma-Aldrich. RBA (76 mer ssDNA, 5′end) modified with biotin-T10 (10 times repeated thymidine bases) were provided by Metabion Inc., (Planegg/Steinkirchen, Germany). The sequence of RBA[15,16] was: 5′-Biotin-TTTTTTTTTTATACCAGCTTAT TCAATTACAGTAGTGAGGGGTCCGTCGTGGGGTAGTTGGGTC GTGGAGATAGTAAGTGCAATCT-3′. Human RBP4 protein (ab114060), anti-RBP4 antibody (ab114062) and RBP4 Human ELISA Kit (ab108897) were purchased from Abcam (Cambridge, USA) and the streptavidin coated polystyrene micro well were provided by Pishtaz Teb Zaman Co. (Tehran, Iran). All chemicals used without further purification. Also in all experiments the solutions were prepared using double distilled deionized water. All the instruments were set to zero with a blank solution to eliminate the interferer substances. A solution containing 150 mM NaCl, 25 mM Tris, 0.1% BSA and 0.05% Tween-20, pH 7.2, was prepared and used as washing solution. Another solution containing 100 mM NaCl, 20 mM Tris–HCl, 2 mM $MgCl_2$, 5 mM KCl, 1 mM $CaCl_2$ and 0.02% Tween-20, pH 7.6, was prepared and used as binding buffer.

Apparatus. Dynamic light scattering (DLS, 90 plus Brookhaven Instruments Corporation, USA) was used for size determination. The single and intercross-linked GNPs images were obtained by PHILIPS CM30 Scanning Transmission Electron Microscope (Philips Electron Optics, Eindhoven, The Netherlands). For UV-Visible spectroscopy, the Cary 100 bio spectrophotometer (Varian, Australia) was used. Attenuated total reflectance-Fourier transform infrared spectroscopy (ATR- FTIR) was performed using Nicolet Nexus 470 FTIR (Nicolet, Madison, WI, USA) spectrometer. IrAnalyze software was also applied for IR spectrum interpretation (LabCognition, Ft. Myers, FL). TMicro centrifuge (Sigma, USA) was used to separate GNPs at different conditions. The samples were centrifuged at 14000 rpm for 30 min at 4 °C. The chemiluminescence emissions were recorded at 425 nm by fluorescence micro plate reader (H4, Bio Tech Co, USA).

Synthesis of GNPs. GNPs were synthesized according to reference No.[27]. Based on the addition of different volume of 1% tri-sodium citrate to $HAuCl_4$ solution, GNPs (Φ: 20–25 nm) were prepared. The resulting particle suspension stocked in a brown bottle at 4 °C.

Preparation of intercross-linked GNPs. As shown in Fig. 3, two different types of modifications were carried out on GNPs: (i) process of A to C for preparation of single GNPs carrying luminol and antibody (L-GNP-Ab) and (ii) process of D to F for preparation of cross-linked GNPs carrying luminol and antibody (L-GNP-Cys-GNP-Ab).

During first process, carboxylated GNPs were prepared in such a way that 1 mL of GNPs was gently added to 2 mL of phosphate buffer solution (PBS, 10 mM, pH 8) containing MUA (3 mM) and Tween-20 (0.2 mg/mL) (Fig. 3A). The mixture was incubated at room temperature for 30 min. The thus prepared carboxylated GNPs

Detection Molecule	Detection method	Signal transduction	Linear range	Detection limit	Assay time	Reference
ssDNA Aptamer	Spectroscopy	Chemiluminescence	0.001–2 ng/mL	951 fg/mL	2 h	Present study
ssDNA Aptamer	Spectroscopy	Surface Plasmon Resonance (SPR)	0.2–0.5 μg/mL	1.58 μg/mL	2 h and 20 mim	[15]
ssDNA Aptamer	Spectroscopy	Enzyme-Linked Antibody-Aptamer Sandwich (ELAAS)	78 ng/mL to 5 μg/mL	75 ng/mL	2 h	[16]
Antibody	Spectroscopy	Enzyme-linked immunosorbent sandwich assay	1–3 ng/mL	>10 ng/mL	4 h and 20 min	[32]
Antibody	Electrochemical	Impedometric	0.01–1000 pg/mL	100 fg/mL	6 h	[23]
Antibody	Spectroscopy	ELISA	6.25–400 ng/mL	6 ng/mL	4 h	(abcam 108897)
Antibody	Mass sensitive	Matrix-Assisted Laser Desorption/Ionization Time-Of-Flight (MALDI-TOF MS)	7.81–500 μg/mL	3.36 μg/mL	46 min	[1]
Antibody	Mass sensitive	Quantitative Mass Spectrometry Immuno-affinity Assay (qMSIA)	7–500 μg/mL	—	46 min	[26]
Antibody	Spectroscopy	Chemiluminescence	1.33 ng/mL	0.62 ng/mL	1 h and 30 min	[33]
Antibody	Spectroscopy	Electro-chemiluminescence	78–5000 ng/mL	26 ng/mL	2 h	[34]

Table 1. Comparison between the parameters obtained by the present biosensor with those methods reported in the literature for determination of RBP4.

Normal Female Samples	*Present Aptasensor	*ELISA μg/mL	Standard Deviation	%CV	Diabetic Female Samples	*Present Aptasensor	*ELISA μg/mL	Standard Deviation	%CV
1	21.738	21.733	0.004	0.018	1	34.893	34.888	0.004	0.011
2	23.73	23.76	0.021	0.088	2	37.001	37.002	0.001	0.002
3	29.9	29.913	0.009	0.03	3	31.353	31.348	0.004	0.012
4	27.1	27.101	0.001	0.003	4	35.46	35.463	0.002	0.005
Average	25.617	25.627	0.009	0.035	Average	34.677	34.675	0.002	0.005

Table 2. Determinations of RBP4 in real (normal and diabetic) female samples by the present aptasensor and ELISA kit. The %CVs for intra- and inter-assay averages are 0.010 and 0.015, respectively. *Mean of triplicate measurements.

Normal Male Samples	*Present Aptasensor	*ELISA μg/mL	Standard Deviation	%CV	Diabetic Male Samples	*Present Aptasensor	*ELISA μg/mL	Standard Deviation	%CV
1	25.834	25.839	0.004	0.015	1	36.496	36.491	0.004	0.011
2	24.045	24.043	0.001	0.004	2	33.93	33.926	0.003	0.008
3	22.942	22.945	0.002	0.008	3	39.681	39.678	0.002	0.005
4	27.443	27.455	0.008	0.029	4	33.559	33.555	0.003	0.009
5	27.235	27.231	0.003	0.011	5	35.711	35.709	0.001	0.003
6	27.043	27.038	0.004	0.014	6	39.89	39.892	0.001	0.002
Average	25.693	25.759	0.004	0.015	Average	36.545	35.693	0.002	0.005

Table 3. Determinations of RBP4 in real (normal and diabetic) male samples by the present aptasensor and ELISA kit. The %CVs for intra- and inter-assay averages are 0.010 and 0.015, respectively. *Mean of triplicate measurements.

were washed with buffer and centrifuged at 14000 rpm for 30 min. Following the careful removing of supernatant, containing excess MUA and Tween 20, the precipitate was re-suspended in buffer. For activation of the carboxylic acid functional groups assembled on GNPs, 1 mL of carboxylated GNPs was added to MES buffer solution (1 mM, pH 5.5) containing 50 μL of EDC (50 mM) and 50 μl of NHS (50 mM) and then, the mixture was incubated at room temperature for 20 min (Fig. 3B). Thereafter, the activated carboxylate GNPs were washed and centrifuged at 14000 rpm for 30 min three times. Finally, the precipitate was re-suspended in PBS. Then 25 μL of polyclonal antibody (20 mg/mL) was added to the activated carboxylate GNPs (Fig. 3C). For immobilizing luminol on antibody bearing GNPs, 200 μL of 10 mM luminol was added to this mixure and the mixture was incubated for 6 hrs at dark in cold room (at 4 °C) with gentle shaking. At the end, the mixture was washed and centrifuged at 14000 rpm for 30 min, three times (Fig. 3D). The prepared luminol-antibody bearing GNPs was diluted in PBS (0.01 M, pH 7.4) and stored at 4 °C.

During the second process, the intercross-linked L-GNP-Cys-GNP-Ab is prepared. For this purpose, according to reference No.[28], cysteine was self-assembled on GNPs (Fig. 3E) and then, one mL of Cys-GNPs was added to two mL of Ab-GNPs. The mixture was incubated for 6 hours at dark in cold room (at 4 °C) with gentle shaking. At the end, the prepared intercross-linked GNPs (GNP-Cys-GNP-Ab) were washed and centrifuged at 7500 rpm for 30 min, three times (Fig. 3F). Finally, in order to conjugate the luminol molecules on intercross-linked GNPs, the free carboxylic acid groups either on cystein or carboxylated GNPs can be linked to amine groups of luminol molecules via EDC and NHS linkers (Fig. 3G). To conjugate the luminol molecules on intercross-linked GNPs, 200 µL of 10 mM luminol was added to 1.5 µL of intercross-linked GNPs and the mixture was incubated for 6 hours at dark in cold room (at 4 °C) with gentle shaking. At the end, the mixture was washed and centrifuged at 7500 rpm for 30 min for three times (Fig. 3H). The prepared L-GNP-Cys-GNP-Ab was diluted in PBS (0.01 M, pH 7.4) and stored at 4 °C.

Immune complex formation and chemiluminescence measurements. As shown in Fig. 3I, streptavidin coated polystyrene micro well was used for biotinylated aptamer immobilization. Firstly, the wells were washed with 200 µL of washing solution and then, 100 µL of 0.4 µM biotinylated aptamer was added into each streptavidin coated polystyrene micro well and incubated for 2 h at room temperature while it was shaking mildly. To remove the non-immobilized reagents, the wells were washed three times. Then, a serial dilution of RBP4 protein in binding buffer was added to the wells[16]. After 1 h, the wells were washed and aptamer-target complexes were incubated with 100 µL of either L-GNP-Ab or L-GNP-Cys-GNP-Ab, while shaking at 25 °C in dark for 1 h. Finally, the wells were washed with 200 µL of washing solution in dark.

The response of aptasensor in PBS containing different concentrations of NaCl were investigated. For chemiluminescence measurements, optimum PBS buffer (pH 8, 0.02 M containing 100 mM NaCl) was added to the immune complex and then $HAuCl_4$ (10 µl, 0.1% w/v) as catalyst and H_2O_2 (10 µL, 10^{-2} M) as initiator were injected to the solution and the chemiluminescence intensity was recorded. Then calibration curve was plotted based on chemiluminescence intensities against the serial dilution of RBP4 protein. Then detection limit (DL) was calculated according to Eq. 3[29]:

$$DL = 3\ S_a/b \tag{3}$$

where, S_a is the standard deviation of the response and b is the slope of the calibration curve.

Feasibility of aptasensor for real samples. The feasibility of present aptasensor for real samples was assessed by 20 serum samples from normal and diabetic individuals, obtained from Tehran University of Medical Sciences. At the same time RBP4 in real samples was determined by the aptasensor and Human ELISA Kit (ab108897) and the results were compared. To verify the reproducibility of responses, the coefficient of variation (%CV) was calculated. First, the standard deviation (σ) was calculated according to Eq. 4[30]:

$$\sigma = \sqrt{\frac{\sum(Result - Mean)^2}{N - 1}} \tag{4}$$

To analyze intra-assay CV, three replicates of three different samples were run in one assay. To analyze inter-assay CV, three different samples were run in three independent assays. The inter or intra-assay variation (%CVs) was calculated using Eq. 5[31]:

$$\%CVs = \sigma/(\text{mean of assay results}) \times 100 \tag{5}$$

The values of %CVs less than 10 and 15, respectively for intra-assay and inter-assay, are generally acceptable.

Ethical approval and informed consent. This study complied with the Declaration of Helsinki (1989 revision) and was approved by the Ethics Committee of the University of Tehran. All of the participants signed an informed consent form before enrollment in the study. All methods and experiments were performed in accordance with the standard ethical guidelines and approved by Ethics Committee of the University of Tehran.

Received: 7 June 2019; Accepted: 30 December 2019;
Published online: 17 January 2020

References

1. Kiernan, U. A., Phillips, D. A., Trenchevska, O. & Nedelkov, D. Quantitative mass spectrometry evaluation of human retinol binding protein 4 and related variants. *PloS one* **6**, e17282, https://doi.org/10.1371/journal.pone.0017282 (2011).
2. Deshpande, A. D., Harris-Hayes, M. & Schootman, M. Epidemiology of Diabetes and Diabetes-Related Complications. *Physical Therapy* **88**, 1254–1264, https://doi.org/10.2522/ptj.20080020 (2008).
3. Kwanbunjan, K. *et al.* Association of retinol binding protein 4 and transthyretin with triglyceride levels and insulin resistance in rural thais with high type 2 diabetes risk. *JBMC Endocrine Disorders* **18**, 26, https://doi.org/10.1186/s12902-018-0254-2 (2018).
4. Wei, Y. *et al.* Serum retinol binding protein 4 is associated with insulin resistance in patients with early and untreated rheumatoid arthritis. *Joint Bone Spine*, https://doi.org/10.1016/j.jbspin.2018.07.002 (2018).
5. Javanbakht, M. *et al.* Cost-of-Illness Analysis of Type 2 Diabetes Mellitus in Iran. *PloS one* **6**, e26864, https://doi.org/10.1371/journal.pone.0026864 (2011).
6. Dorcely, B. *et al.* Novel biomarkers for prediabetes, diabetes, and associated complications. *Diabetes, metabolic syndrome and obesity: targets and therapy* **10**, 345–361, https://doi.org/10.2147/DMSO.S100074 (2017).
7. Rocha, M. *et al.* Association of serum retinol binding protein 4 with atherogenic dyslipidemia in morbid obese patients. *PloS one* **8**, e78670, https://doi.org/10.1371/journal.pone.0078670 (2013).
8. Takebayashi, K., Suetsugu, M., Wakabayashi, S., Aso, Y. & Inukai, T. Retinol binding protein-4 levels and clinical features of type 2 diabetes patients. *The Journal of Clinical Endocrinology & Metabolism* **92**, 2712–2719 (2007).

9. Muoio, D. M. & Newgard, C. B. Metabolism: A is for adipokine. *Nature* **436**, 337–338, https://doi.org/10.1038/436337a (2005).
10. Moraes-Vieira, P. M. *et al.* RBP4 activates antigen-presenting cells, leading to adipose tissue inflammation and systemic insulin resistance. *Cell metabolism* **19**, 512–526, https://doi.org/10.1016/j.cmet.2014.01.018 (2014).
11. Graham, T. E., Wason, C. J., Bluher, M. & Kahn, B. B. Shortcomings in methodology complicate measurements of serum retinol binding protein (RBP4) in insulin-resistant human subjects. *Diabetologia* **50**, 814–823, https://doi.org/10.1007/s00125-006-0557-0 (2007).
12. Polyzos, S. A., Kountouras, J., Anastasilakis, A. D., Geladari, E. V. & Mantzoros, C. S. Irisin in patients with nonalcoholic fatty liver disease. *Metabolism: clinical and experimental* **63**, 207–217, https://doi.org/10.1016/j.metabol.2013.09.013 (2014).
13. Lee, J. O. *et al.* Aptamers as molecular recognition elements for electrical nanobiosensors. *Analytical and bioanalytical chemistry* **390**, 1023–1032, https://doi.org/10.1007/s00216-007-1643-y (2008).
14. Song, S., Wang, L., Li, J., Zhao, J. & Fan, C. Aptamer-based biosensors. *Trends in Analytical Chemistry* **27**, 108–117 (2008).
15. Lee, S. J. Y. *et al.* ssDNA aptamer-based surface plasmon resonance biosensor for the detection of retinol binding protein 4 for the early diagnosis of type 2 diabetes. *Analytical chemistry* **80**, 2867–2873, https://doi.org/10.1021/ac800050a (2008).
16. Lee, S. J., Park, J. W., Kim, Y. S., Youn, B. S. & Gu, M. B. Sensitive detection of adipokines for early diagnosis of type 2 diabetes using enzyme-linked antibody-aptamer sandwich (ELAAS) assays. *Sensors and Actuators B: Chemical* **168**, 243–248 (2012).
17. Liu, X., Atwater, M., Wang, J. & Huo, Q. Extinction coefficient of gold nanoparticles with different sizes and different capping ligands. *Colloids and Surfaces B: Biointerfaces* **58**, 3–7, https://doi.org/10.1016/j.colsurfb.2006.08.005 (2007).
18. Liu, Y. *et al.* Delivery of vincristine sulfate-conjugated gold nanoparticles using liposomes: a light-responsive nanocarrier with enhanced antitumor efficiency. *International journal of nanomedicine* **10**, 3081–3095, https://doi.org/10.2147/IJN.S79550 (2015).
19. Li, F. & Cui, H. A label-free electrochemiluminescence aptasensor for thrombin based on novel assembly strategy of oligonucleotide and luminol functionalized gold nanoparticles. *Biosens Bioelectron* **39**, 261–267, https://doi.org/10.1016/j.bios.2012.07.060 (2013).
20. Zhang, Z. F., Cui, H., Lai, C. Z. & Liu, L. J. Gold nanoparticle-catalyzed luminol chemiluminescence and its analytical applications. *Analytical chemistry* **77**, 3324–3329, https://doi.org/10.1021/ac050036f (2005).
21. Yadav, R., Berlina, A. N., Zherdev, A. V. & Dzantiev, B. B. Chemiluminescence catalysed by gold nanoparticles for the analysis of arsenic (III) in real water AU - Gaur, Mulayam Singh. *Journal of Experimental Nanoscience* **11**, 1372–1383, https://doi.org/10.1080/17458080.2016.1227096 (2016).
22. Sabouri, S., Ghourchian, H., Shourian, M. & Boutorabi, M. A gold nanoparticle-based immunosensor for the chemiluminescence detection of the hepatitis B surface antigen. *Analytical Methods* **6**, 5059–5066, https://doi.org/10.1039/c4ay00461b (2014).
23. Paul, A., Chiriaco, M. S., Primiceri, E., Srivastava, D. N. & Maruccio, G. Picomolar detection of retinol binding protein 4 for early management of type II diabetes. *Biosens Bioelectron* **128**, 122–128, https://doi.org/10.1016/j.bios.2018.12.032 (2018).
24. Han, K., Liang, Z. & Zhou, N. Design strategies for aptamer-based biosensors. *Sensors (Basel)* **10**, 4541–4557, https://doi.org/10.3390/s100504541 (2010).
25. Zichel, R., Chearwae, W., Pandey, G. S., Golding, B. & Sauna, Z. E. Aptamers as a sensitive tool to detect subtle modifications in therapeutic proteins. *PloS one* **7**, e31948, https://doi.org/10.1371/journal.pone.0031948 (2012).
26. Yang, Q. *et al.* Quantitative measurement of full-length and C-terminal proteolyzed RBP4 in serum of normal and insulin-resistant humans using a novel mass spectrometry immunoassay. *Endocrinology* **153**, 1519–1527, https://doi.org/10.1210/en.2011-1750 (2012).
27. Frens, G. Controlled Nucleation for the Regulation of the Particle Size in Monodisperse Gold Suspensions. *nature physical science* **241**, 20–22 (1973).
28. Aryal, S., Dharmaraj, N., Bhattarai, N., Kim, C. H. & Kim, H. Y. Spectroscopic identification of S-Au interaction in cysteine capped gold nanoparticles. *Spectrochimica acta. Part A, Molecular and biomolecular spectroscopy* **63**, 160–163, https://doi.org/10.1016/j.saa.2005.04.048 (2006).
29. Shrivastava, A. & Gupta, V. Methods for the determination of limit of detection and limit of quantitation of the analytical methods. *Chronicles of Young Scientists* **2**, 21–21 (2011).
30. Reed, G. F., Lynn, F. & Meade, B. D. Use of coefficient of variation in assessing variability of quantitative assays. *Clin Diagn Lab Immunol* **9**, 1235–1239, https://doi.org/10.1128/cdli.9.6.1235-1239.2002 (2002).
31. Jaedicke, K. M., Taylor, J. J. & Preshaw, P. M. Validation and quality control of ELISAs for the use with human saliva samples. *Journal of Immunological Methods* **377**, 62–65, https://doi.org/10.1016/j.jim.2012.01.010 (2012).
32. Lee, N. S. *et al.* Development of a mouse IgA monoclonal antibody-based enzyme-linked immunosorbent sandwich assay for the analyses of RBP4. *Sci Rep* **8**, 2578, https://doi.org/10.1038/s41598-018-20762-x (2018).
33. Ying, W. & Lili, C. Quantitative determination RBP4 kit by chemiluminescence magnetic enzymoimmune method (2013).
34. Wu, B. *et al.* Sensitive ECL immunosensor for detection of retinol-binding protein based on double-assisted signal amplification strategy of multiwalled carbon nanotubes and Ru(bpy)32+ doped mesoporous silica nanospheres. *Biosensors and Bioelectronics* **50**, 300–304, https://doi.org/10.1016/j.bios.2013.06.045 (2013).

Acknowledgements

Financial support provided by the Research Council of the University of Tehran is gratefully appreciated.

Author contributions

R. Torabi conceived and conducted the experiments and H. Ghourchian analyzed the results. Both authors wrote and reviewed the manuscript.

Competing interests

The authors declare no competing interests.

Additional information

Correspondence and requests for materials should be addressed to H.G.

Reprints and permissions information is available at www.nature.com/reprints.

Publisher's note Springer Nature remains neutral with regard to jurisdictional claims in published maps and institutional affiliations.